Extended Abstracts of the 2015 International Conference on Solid State Devices and Materials, Sapporo, 2015, pp620-621

Stretchable Photonic Crystal Coupled-Nanobeam Lasers for Stretch Sensing

Chun Wang*, Tsan-Wen Lu, and Po-Tsung Lee

Department of Photonics, National Chiao Tung University
Rm. 401 CPT Building, 1001 Ta-Hsueh Road, Hsinchu 30010, Taiwan
Phone: +886-3-5712121 ext. 59341 E-mail: a60912game@hotmail.com

Abstract

We design and demonstrate stretchable nanolasers based on photonic crystal coupled-nanobeams with extremely small device footprint embedded in polydimethylsiloxane. In addition to identifying the bonding and anti-bonding lasing modes, the minimum detectable stretch of 1% is achieved via the bonding mode.

1. Introduction

Recently, various photonic crystal (*PhC*) devices on flexible substrates [1,2] have been proposed and demonstrated for different functionalities, for example, photonic integrated circuits (*PICs*), tunable optical filters, stretch and curvature sensors, and so on. This kind of flexible devices is beneficial for the components in micro-electro-mechanical systems, and could be the pioneer components for the future flexible lab-on-chip. Among these functionalities, stretch and curvature sensors [3,4] attract lots of attention owing to their practicalities in strain and stress monitoring in different architectures. Most reported devices employee *2D PhCs* consisted of rods to avoid device cracking under stretching and bending. However, *2D PhCs* lead to large device footprints and show low compatibility with waveguide-based *PICs*. In addition, discontinuous rods are not beneficial for current injection for active type sensors.

In this report, we propose and demonstrate *1D PhC* coupled-nanobeam nanocavities (*CNB-ncs*) embedded in polydimethylsiloxane (*PDMS*). This design with simple topology not only results in very small device footprint but also avoids device cracking under stretch. In addition to laser actions, high stretch sensitivity is also achieved via our presented design both in simulations and experiments.

2. Design and Characteristics of *PhC CNB-ncs* in *PDMS*

Design of PhC CNB-ncs

Our proposed *PhC CNB-ncs* consists of two identical *PhC NBs* side by side, as shown in Fig. 1(a). Periodic air holes are manufactured on each *NB* to form *1D PhCs*. And the lattice constant of *PhCs* is gradually increased (5 nm increment) from the center to the both sides of *NB*, while the radii of all air holes are fixed. These gradually-varied *PhCs* form a double-hetero structure with mode gap effect, which produce a nanocavity, as shown in Fig. 1(a). The gap size *g* defined in Fig. 1(a) is chosen to be smaller than 200 nm for producing strong coupling between the nanocavities.

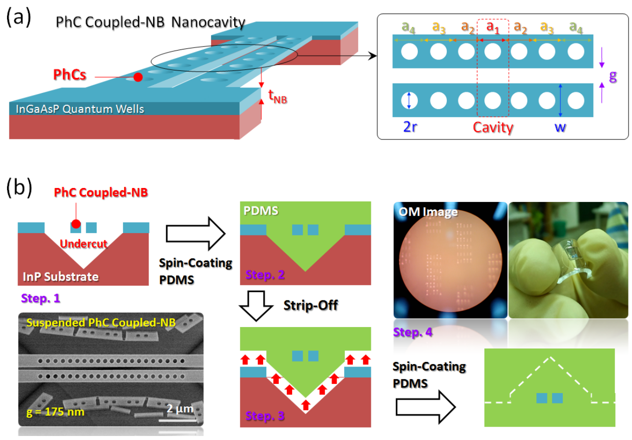

Fig. 1 (a) Schematic and parameter definitions of *PhC CNB-ncs*. (b) Fabrication process of embedding *PhC CNB-ncs* in PDMS. *SEM* picture of *PhC CNB-ncs* before embedding in *PDMS*, *OM* image and sample photo after embedding are also shown in (b).

Manufacturing PhC CNB-ncs in Stretchable PDMS

To embed *PhC CNB-ncs* in stretchable material, we apply *PDMS* (with low refractive index of 1.4) stamping process, as illustrated in Fig. 1(b). In Step 1, suspended *PhC CNB-ncs* (composed of *InGaAsP* quantum wells) are prepared via a series of electron-beam lithography and dry/wet etching processes [5]. The top-view scanning electron microscope (*SEM*) picture is shown as the inset of Step 1 in Fig. 1(b). In Step 2 we then directly spin-coating *PDMS* on the devices. The infiltration of *PDMS* into the device undercut guarantees the success in the following strip-off process. The device with *PDMS* is then softly baked at 60˚C for 6 hours. In Step 3, the baked *PDMS* with *PhC CNB-ncs* is directly stripped-off from the *InP* substrate. In Step 4, the stripped-off *PDMS* is then spin-coated a *PDMS* thin film to smooth its surface. The optical microscopic (*OM*) image and sample photo of the *PhC CNB-ncs* in *PDMS* are shown as the insets of Step 4 in Fig. 1(b). The former one reveals high success ratio of this process and the latter one shows the flexibility of *PhC CNB-ncs* in *PDMS*.

Stretchable PhC CNB-ncs Lasers for Stretch Sensing

To identify the modes of *PhC CNB-ncs* in *PDMS*, *3D* finite-element method (*COMSOL* Multiphysics software package) is utilized. Theoretically, this *PhC CNB-ncs* forms a photonic molecule with optical bonding and anti-binding modes analog to the energy states in a two-atom system. In Fig. 2(a), simulated wavelength variations of the bonding

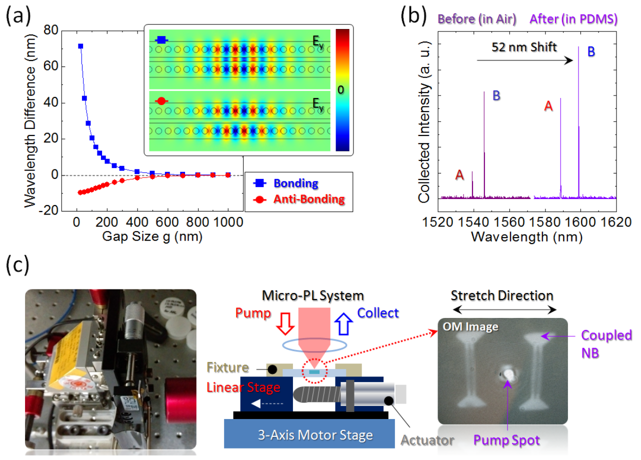

Fig. 2 (a) Theoretical wavelengths of bonding and anti-bonding modes in *PhC CNB-ncs* with different *g* embedded in *PDMS*. (b) Lasing spectra of *PhC CNB-ncs* with g = 175 nm before and after being embedded in *PDMS*. (c) Picture and schematic of stretch stage for stretchable *PhC CNB-ncs* lasers measurement. The *OM* image of *PhC CNB-ncs* in *PDMS* is also shown in (c).

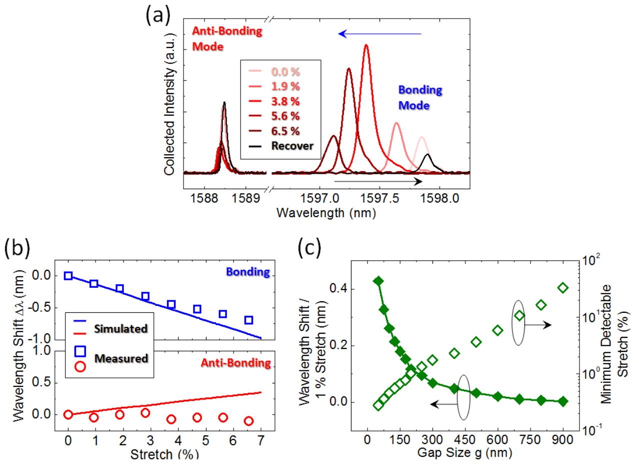

Fig. 3 (a) Lasing spectra, (b) measured and simulated wavelength shifts of bonding and anti-bonding modes under different stretches. (c) Theoretical wavelength shift under 1% stretch and the minimum detectable stretch of bonding mode in *PhC CNB-ncs* with different *g*.

and anti-bonding modes in *PhC CNB-ncs* with different *g* reveal above feature. In addition, the bonding mode shows larger wavelength shift than that of anti-bonding mode when *g* is changed. Theoretical bonding and anti-bonding mode profiles in E_y fields when g = 175 nm are shown as the insets of Fig. 2(a).

In our micro-photoluminescence (micro-*PL*) measurement system, *PhC CNB-ncs* in *PDMS* (with g = 175 nm) is excited at room temperature by 15 ns optical pulse. Lasing spectrum from bonding and anti-bonding modes is shown in Fig. 2(b). The measured bonding and anti-bonding mode lasing from *PhC CNB-ncs* before being embedded in *PDMS* is also shown in Fig. 2(b). A significant wavelength red shift of 52 nm attributed to the increased index caused by *PDMS* is observed, which agrees well with the simulated value of 56 nm.

To characterize the stretch ability of *CNB-ncs* in *PDMS*, we setup a stretch stage in our micro-*PL* system, as shown in Fig. 2(c). This stage consists of a 3-axis motor stage for controlling device position and a linear stage for stretching the device. The *OM* image of *PhC CNB-ncs* in *PDMS* is also shown as the inset of Fig. 2(c). The stretch direction is perpendicular to the *CNB*. The measured bonding and anti-bonding mode lasing spectra from *PhC CNB-ncs* in *PDMS* (with g = 175 nm) under different stretches from 0 to 6.5% are shown in Fig. 3(a). The bonding mode shows large blue shift of 0.7 nm in wavelength, which is caused by the increased *g* when stretching the device. Considering its spectral line-width of 0.12 nm, the minimum detectable stretch is 1%. The bonding mode wavelength variation trend under different stretches quite agrees with the simulation results, as shown in Fig. 3(b). In contrast, under different stretches, the anti-bonding mode is almost invariant. When *g* increases, the anti-bonding mode shows very small red shift in wavelength. And this red shift will be slightly compensated by a blue shift in wavelength owing to the decreased index of *PDMS* under stretching.

In addition, for *PhC CNB-ncs* with different *g*, we also calculate the wavelength shift under 1% stretch and minimum detectable stretch of bonding mode, as shown in Fig. 3(c). Suppose the lasing mode spectral line-width is 0.12 nm, the minimum detectable stretch is as small as 0.3% when g = 50 nm.

3. Conclusions

In this report, we design and demonstrate stretchable nanolasers based on *PhC CNB-ncs* embedded in *PDMS*. In addition to identifying the bonding and anti-bonding lasing modes, the minimum detectable stretch of 1% is achieved via bonding mode in our presented design when g = 175 nm both in simulation and experiment. Theoretically, the minimum detectable stretch can be further improved to be 0.3% by decreasing *g* to be 50 nm. This design with simple and continuous topology not only shows very small device footprint but also avoids device cracking under stretch. Moreover, the *NB* design shows high compatibility with waveguide-based *PICs*. Therefore, we believe our presented *PhC CNB-ncs* embedded in *PDMS* has great potential for realizing highly sensitive on-chip stretch sensors.

References

[1] J. Hu, L. Li, H. Lin, P. Zhang, W. Zhou, and Z. Ma, Opt. Mater. Express **3** (2013) 1313.

[2] S. Walia, C. M. Shah, P. Gutruf, H. Nili, D. R. Chowdhury, W. Withayachumnankul, M. Bhaskaran, and S. Sriram, Appl. Phys. Rev. **2** (2015) 011303.

[3] K. S. Hsu, T. T. Chiu, P. T. Lee, and M. H. Shih, J. Lightwave Technol. **31** (2013) 1960.

[4] C. L. Yu, H. Kim, N. de Leon, I. W. Frank, J. T. Robinson, M. McCutcheon, M. Liu, M. D. Lukin, M. Lončar, and H. Park, Nano Lett. **13** (2013) 248.

[5] P. T. Lee, T. W. Lu, and L. H. Chiu, J. Lightwave Technol. **31** (2013) 36.